

Large effect QTL explain natural phenotypic variation for the developmental timing of vegetative phase change in maize (*Zea mays* L.)

Jillian M. Foerster · Timothy Beissinger ·
Natalia de Leon · Shawn Kaeppler

Received: 6 June 2014 / Accepted: 20 December 2014 / Published online: 10 January 2015
© Springer-Verlag Berlin Heidelberg 2015

Abstract

Key message Natural variation for the timing of vegetative phase change in maize is controlled by several large effect loci, one corresponding to *Glossy15*, a gene known for regulating juvenile tissue traits.

Abstract Vegetative phase change is an intrinsic component of developmental programs in plants. Juvenile and adult vegetative tissues in grasses differ dramatically in their anatomical and biochemical composition affecting the utility of specific genotypes as animal feed and biofuel feedstock. The molecular network controlling the process of developmental transition is incompletely characterized. In this study, we used scoring for juvenile and adult epicuticular wax as an entry point to discover quantitative trait loci (QTL) controlling phenotypic variation

for the developmental timing of juvenile to adult transition in maize. We scored the last leaf with juvenile wax on 25 recombinant inbred line families of the B73 reference Nested Association Mapping (NAM) population and the intermated B73×Mo17 (IBM) population across multiple seasons. A total of 13 unique QTL were identified through genome-wide association analysis across the NAM populations, three of which have large effects. A QTL located on chromosome nine had the most significant SNPs within *Glossy15*, a gene controlling expression of juvenile leaf traits. The second large effect QTL is located on chromosome two. The most significant SNP in this QTL is located adjacent to a homolog of the *Arabidopsis* transcription factor, *enhanced downy mildew-2*, which has been shown to promote the transition from juvenile to adult vegetative phase. Overall, these results show that several major QTL and potential candidate genes underlie the extensive natural variation for this developmental trait.

Communicated by Jianbing Yan.

Electronic supplementary material The online version of this article (doi:10.1007/s00122-014-2451-3) contains supplementary material, which is available to authorized users.

J. M. Foerster · T. Beissinger · N. de Leon · S. Kaeppler (✉)
Department of Agronomy, University of Wisconsin-Madison,
1575 Linden Dr., Madison, WI 53706, USA
e-mail: smkaeppl@wisc.edu

Present Address:

J. M. Foerster
DuPont Pioneer, Johnston, IA 50131, USA

T. Beissinger
Department of Animal Science, University of Wisconsin-Madison,
1675 Observatory Dr., Madison, WI 53706, USA

N. de Leon · S. Kaeppler
DOE Great Lakes Bioenergy Research Center,
1552 University Avenue, Madison, WI 53706, USA

Introduction

Heteroblasty is defined as the production of different qualitative structures at different times throughout plant development (Zotz et al. 2011). In maize, this involves two processes: shoot maturation or phase change as well as physiological aging (Bongard-Pierce et al. 1996). Maize development consists of three phases including the juvenile vegetative, adult vegetative, and reproductive. The transition to adult vegetative tissue is required prior to the reproductive transition and is under independent, yet overlapping genetic control (Huijser and Schmid 2011). In maize, the earliest developed leaves are composed completely of juvenile tissue, followed by a few or several transition leaves, and the uppermost leaves are composed entirely of



Fig. 1 Maize transition leaves. Juvenile leaf tissue is distinguished by the presence of epicuticular wax, which has a dull, blueish appearance. Dark, glossy green portions of the leaf are adult tissue. **a** Completely juvenile leaf. **b** Transition leaf. **c** Last leaf with epicuticular wax (LLEW)

adult tissue (Fig. 1). Juvenile and adult tissues are distinguished by differences in epidermal cell shape, cell type, wax and trichome production, cell wall histochemistry, photosynthetic capacity as well as disease resistance (Lawson and Poethig 1995; Bongard-Pierce et al. 1996; Poethig 2003). Juvenile leaves produce epicuticular wax, lack epidermal hairs and bulliform cells, but have a thin (1 μm) cuticle. In contrast, adult tissue does not produce epicuticular wax but has epidermal hairs, a thick (3 μm) cuticle, and bulliform cells. Internodes associated with juvenile leaves are more compressed and are capable of producing adventitious roots from lateral buds, whereas adult internodes are more elongated and lateral buds are either absent or form ears. Transition leaves produce a combination of juvenile and adult traits with juvenile tissue at the tip of the leaf and adult tissue near the base. The reproductive phase, which is well characterized and whose genetic control has been studied extensively, is defined by the production of the terminal inflorescence or the tassel and axillary reproductive structures and the ear primordia.

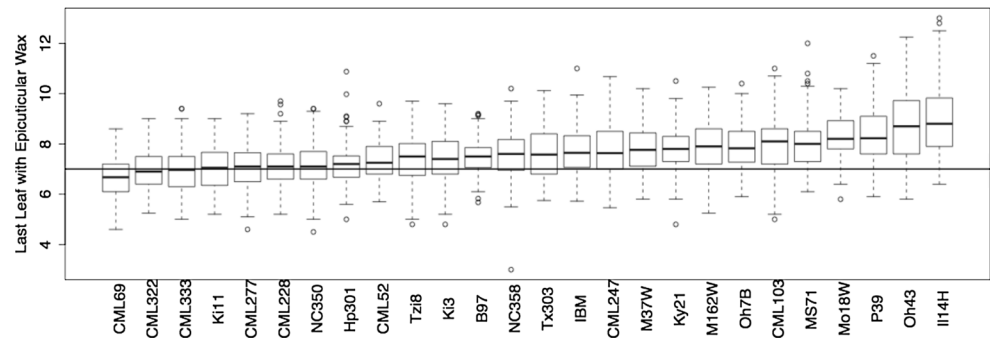
Extensive natural variation in maize for the timing of developmental transitions exists and has been linked to several important agronomic traits such as resistance to insects and common rust (Riedeman et al. 2008). In a divergent recurrent selection experiment, Riedeman et al. (2008) found that feeding damage from European corn borer was significantly greater in the late phase change population and significantly correlated with the last leaf with epicuticular wax.

The duration of juvenility, and thereby proportion of juvenile and adult tissue, may also have an impact on overall tissue recalcitrance in the context of lignocellulosic biofuel production due to differences in cell wall sugar composition as well as the availability of these sugars for saccharification. Lignin can prevent sugar release in cell walls and previous studies have shown that epidermal cells in adult leaves have higher lignin levels compared to juveniles leaves (Evans et al. 1994). Abedon et al. (2006) also found that juvenile leaf tissue contained higher levels of total uronosyls acids, arabinose, and galactose, which are components of pectin. In addition, transgenic switchgrass plants with the maize *Corngrass1* (*Cg1*) mutation, which promotes juvenile characteristics, had higher glucose release from saccharification (Chuck et al. 2011). Most of the epidermal traits of the vegetative stages are well studied and characterized due to their ease of visibility; however, the genetic control of this phase change is not well understood.

The transitional stages of the tissues produced during vegetative phase change and reproductive phase change, as well as the phenotypes of mutants affecting these processes, show that the phases of development are under independent, yet overlapping genetic regulation (Poethig 1990). *Teopod 1*, 2, and 3 (*Tp1*, *Tp2*, *Tp3*) and *Cg1* are gain-of-function mutants that all extend the juvenile phase but do not necessarily affect flowering time. In *Tp2* plants, the reproductive phase is initiated at the same time as the wild-type plants despite the extended juvenile phase, while *Cg1* mutants have been observed to have delayed, abnormal floral structures, or to not flower at all (Lawson and Poethig 1995; Chuck et al. 2011).

MicroRNAs play an important role in regulating the timing of plant developmental transitions. By regulating transcripts of developmental genes, miRNAs control some aspects of leaf morphology, polarity and floral organ identity, and some stress responses (Willmann and Poethig 2005) as well as the timing of juvenile to adult vegetative phase change. The maize and *Arabidopsis* signaling pathway and miRNA expression cascade are very similar (Nonogaki 2010). In maize, the *Cg1* mutant retains juvenile traits resulting in initiation of tillers at each leaf axil causing a bush-like appearance. This phenotype is due to the ectopic overexpression of two tandem miR156 genes (Chuck et al. 2007). miR156 targets SQUAMOSA PROMOTER BINDING PROTEIN-LIKE transcription factors (SPL) such as *teosinte glume architecture1* (*tga1*) in maize and SPL13 in *Arabidopsis*. SPL transcription factors upregulate miR172 in both species and miR172 targets AP2-like transcription factors, such as *glossy15* (*gl15*) in maize and *SCHNARCHSAPFEN* (*SNZ*) in *Arabidopsis*. *Glossy15* maintains expression of juvenile traits in the leaf epidermis and suppresses adult traits. Mutants of *gl15* show

Fig. 2 Phenotypic variation for last leaf with epicuticular wax (LLEW) by population. Nested Association Mapping (NAM) families are labeled by the non-B73 parent. The horizontal solid line at leaf 7 represents the average LLEW of B73



premature vegetative phase change to the adult state (Evans et al. 1994). In *Cgl* mutants of maize, the overexpression of miR156 causes a decrease in *tgal* and miR172 (Chuck et al. 2007), which then causes an increase in expression of *gl15*. In addition to this miRNA cascade, the pathway for siRNA biogenesis is also involved in the control of vegetative phase change including the *HASTY*, *ZIPPER*, *SGS3*, and *RDR6* siRNA genes of *Arabidopsis* (Bollman et al. 2003; Peragine et al. 2004).

Analysis of natural variation provides the possibility to characterize the role of known genes in controlling quantitative variation, and the potential to discover novel genes and alleles. The goal of this study was to characterize QTL controlling the timing of juvenile to adult transition in maize using the uppermost leaf with juvenile wax as an indicator trait.

Results

Phenotypic assessment of vegetative phase change

Vegetative phase change was scored by identifying the last leaf with epicuticular wax in the B73 reference Nested Association Mapping (NAM) (Buckler et al. 2009) and the Intermated B73×Mo17 (IBM) (Lee et al. 2002) recombinant inbred line (RIL) populations grown in West Madison and Arlington, WI in 2008 and 2009. The last leaf with juvenile epicuticular wax (last leaf with epicuticular wax abbreviated LLEW) varied in the NAM RILs from leaf 4.5 to leaf 13.25 with an overall repeatability of 0.50 (Fig. 2). By-population repeatability for the NAM families ranged from 0.24 to 0.64 with a mean of 0.53 (Supplemental Table 1). The phenotypic distribution of the NAM families is centered near leaf 7, which is the average LLEW of B73, the common parent among the NAMs. The last leaf with epicuticular wax ranged from leaf 5.4 to 11 in the IBM RILs with a heritability of 0.60 (Fig. 2). Although node number is highly correlated with flowering time, LLEW was found to have a low correlation with days to silk, days to pollen shed, or node number with Pearson correlation

coefficients of -0.16 , -0.18 , and 0.10 (Supplemental Fig. 1), respectively, across the NAM families suggesting different underlying genetic mechanisms controlling natural variation for these developmental traits.

Genetic dissection of vegetative phase change

A total of 13 QTL were identified through joint linkage mapping (Buckler et al. 2009) that collectively explain 50.2 % of the total phenotypic variation (Fig. 3; Supplemental Table 2). Three major QTL located on chromosomes two, three, and nine had LOD scores of 303.9, 87.5 and 141.2, respectively. The difference between a predicted individual with all early alleles at these three loci relative to one with all late alleles is ~4 days (Fig. 4). Interestingly, based on joint linkage analysis, the additive effect of all non-B73 alleles at the chromosome two QTL across 22 significant NAM families extends the juvenile phase compared to B73 while there are positive and negative parental allelic contrasts for the other two QTL.

The NAM design combined with increased marker density from HapMap1 (Gore et al. 2009) allows for further resolution of QTLs through a genome-wide association (GWAS) scan. GWAS was performed as in Tian et al. (2011). Ninety-one significant associations were detected with the subsampling method using a BPP threshold of 0.05 (Fig. 3). At the QTL near marker m984 (93.4 Mb) on chromosome nine, one SNP was present in 97 out of 100 subsample models and had an LOD score of 73 using single-marker analysis. This SNP lies within the gene *gl15* (GRMZM2G160730), which controls the expression of juvenile leaf traits (Table 1). At the QTL near marker m298 (234.2 Mb) on chromosome two, a large cluster of eight significant associations spanned a distance of 920 kb that included an EDM2-like gene (GRMZM2G362718) and a gene annotated as Argonaute 14 (GRMZM2G059033). Eighty-five percent of the subsampling models included one of these SNPs, which is located 690 bp downstream of the GRMZM2G362718, a homolog of *Arabidopsis* EDM2, and 15 % of the models included an SNP located within the gene model (Table 1). Additionally, 2 Mb upstream of

Fig. 3 GWAS results for last leaf with epicuticular wax (LLEW) using the Nested Association Mapping (NAM) population. *Black dashed lines* indicate NAM joint linkage QTL peaks; scale, LOD. *Green lines* indicate IBM composite interval mapping QTL support intervals; scale, LOD. *Triangles* are significant associations identified in NAM subsampling GWAS; scale, RMIP. *Blue downward pointing triangles* have a mean negative effect (58 SNPs) while red upward pointing triangles have a mean positive effect (33 SNPs). Additive effects are relative to B73

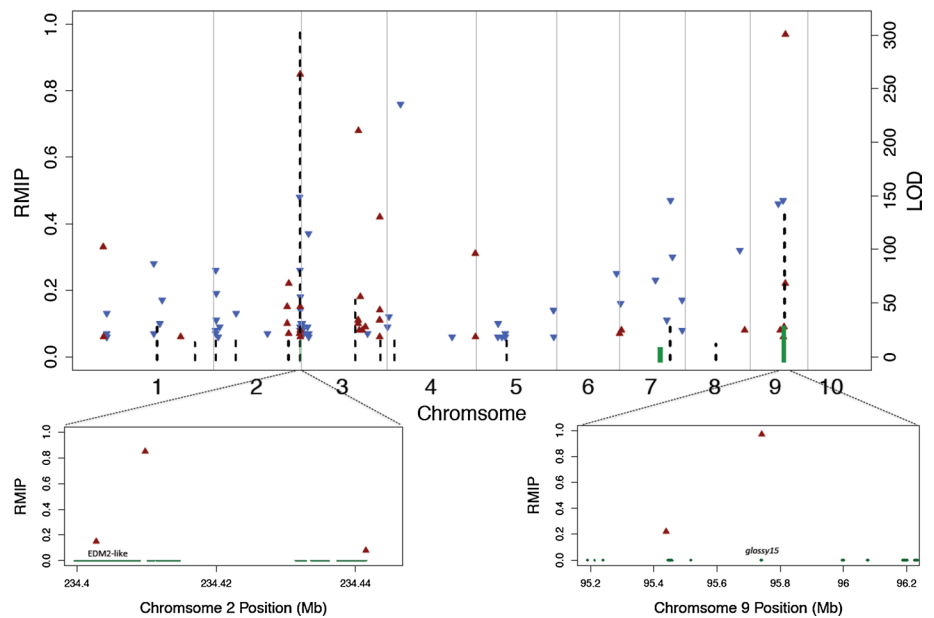
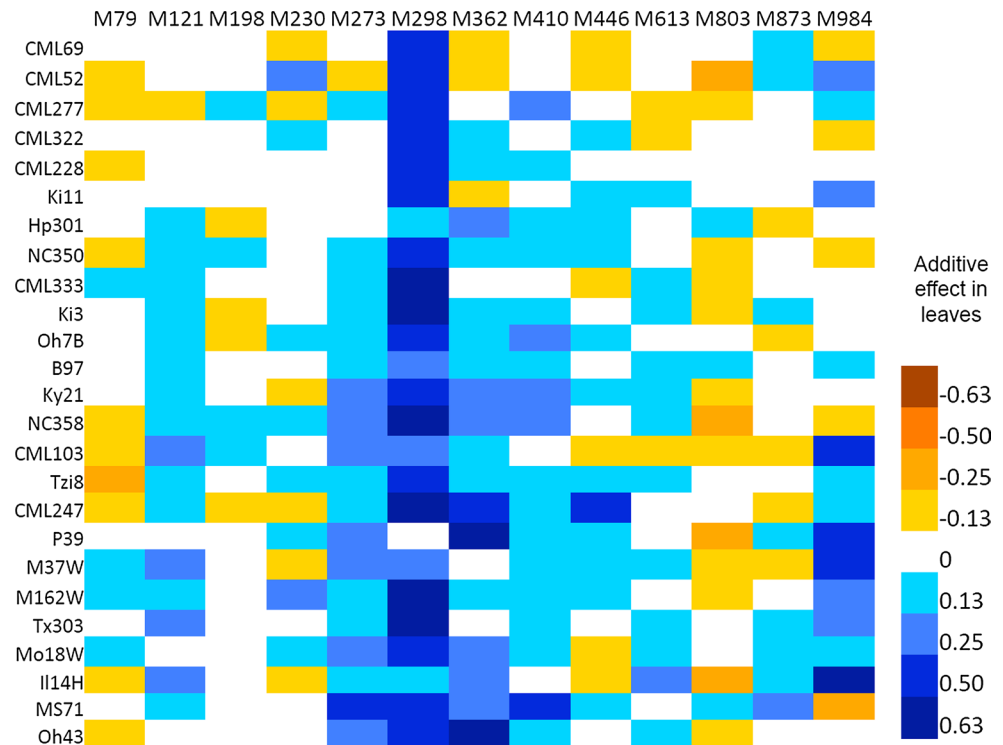


Fig. 4 Heat map for transition QTL effects by Nested Association Mapping (NAM) family. Additive effects are relative to B73. Combining the most extreme allele at each of the three most significant loci (M298, M362, and M984) equates to a 4 leaf difference in transition, which is ~40 % of the variation observed across all NAM populations



the EDM2-like gene, an SNP at 232.7 Mb on chromosome two is present in 48 % of the subsampling models. However, the average allele effect for this SNP is in the opposite direction compared to the SNP at 234.4 Mb. Although physically close, these two SNPs are not in high linkage disequilibrium ($r^2 = 0.02$) and are segregating in different populations.

Two significant regions detected in this study are located in close proximity to SPL-like genes, which are direct targets

of miR156. A region on chromosome five, near marker m613 (81.9 Mb), contains two SNPs that are each 19.2 kb downstream of an SPL12-like gene (GRMZM2G097275). Additionally, another SNP located on chromosome five at 58.0 Mb is located 2.8 kb downstream of an SPL11-like gene (GRMZM2G414805). cDNA sequences of both GRMZM2G097275 and GRMZM2G414805 contain miR156-binding sites (Supplemental Fig. 2a, b) but have not been experimentally proven targets of this microRNA.

Table 1 SNPs and candidate genes significantly associated with the last leaf with epicuticular wax (LLEW)

Candidate gene	Annotation	Chr	Transcript start	Transcript stop	SNP position	SNP distance from gene (bp)	P value	Mean additive effect
GRMZM2G059033	Argonaute 14	2	232,715,202	232,722,126	232,721,405	In gene model	3.77E ⁻¹⁴	−0.43
GRMZM2G362718	EDM2; transcription factor	2	234,399,642	234,409,121	234,409,811	690 Downstream	1.04E ⁻¹⁹⁸	0.50
GRMZM2G106613	Flowering time protein isoform beta	3	154,660,653	154,670,278	154,661,767	In gene model	1.33E⁻³⁰	0.45
GRMZM2G160971	Ap2 domain protein	3	212,501,261	212,503,692	212,462,585	38,676 Upstream	1.52E⁻⁰⁸	0.13
GRMZM2G414805	Squamosa promoter-binding 11	5	58,055,907	58,060,567	58,053,076	2,831 Upstream	1.63E ⁻⁰⁷	0.16
GRMZM2G097275	Squamosa promoter-binding 12	5	77,940,665	77,945,714	77,921,406	19,259 Upstream	2.95E ⁻⁰⁸	−0.18
GRMZM2G160730	Glossy15	9	95,739,337	95,742,689	95,741,728	In gene model	2.60E ⁻⁵⁶	0.59

Candidate genes are plausible biological genes in the locus or an adjacent annotated gene model. Lines highlighted in bold were identified as flowering time QTL in a previous study (Buckler et al. 2009)

The two QTL located on chromosome three at markers m363 (149.2 Mb) and m410 (214.3 Mb) were also detected as flowering time QTL in a previous NAM study (Buckler et al. 2009). Sixty-eight percent of subsampling models included an SNP on chromosome three at 154.6 Mb which is located within a gene encoding the maize ortholog of the flowering time gene LUMINIDEPENDENS from Arabidopsis (GRMZM2G106613). However, the role of this protein in maize flowering remains unclear (van Nocker et al. 2000). Four SNPs span the second region on chromosome three and this region contains an AP2-domain containing protein. Two of the SNPs are 38.6 kb upstream of this gene (GRMZM2G160971) and at least one SNP is present in 56 % of subsampling models (Table 1).

Composite interval mapping was performed with 302 inbred lines of the IBM population using 1,340 markers. QTL were detected on chromosomes two, seven, and nine explaining 15.2, 7.4, and 23.4 % of the variation, respectively. The QTL on chromosomes two and nine had the largest additive effects of 0.38 and −0.47 leaves, respectively. Based on overlapping LOD support intervals, the QTL on chromosomes two (M298) and nine (M984) are co-located with the QTL detected in the NAM joint-linkage mapping analysis. The QTL detected on chromosome seven in the IBM population is approximately 20 Mb upstream of the NAM chromosome seven QTL (Fig. 3).

Glossy15 allelic diversity characterization

The most significant SNP identified through GWAS analysis is located at 95,741,728 bp on chromosome 9 in the 9th

Table 2 HapMap SNPs causing amino acid changes in the proteins of *Glossy15* and GRMZM2G362718

	Amino acid substitution	Causal SNP location	SNP alleles
Glossy15	G15S	95,739,756	T/A
	L26R	95,739,788	T/G
	V37E	95,739,821	T/A
	F45L	95,739,846	C/G
	P69A	95,739,916	C/G
	V85M	95,739,964	G/A
GRMZM2G362718	P511R	234,406,954	C/G
	E656K	234,407,771	G/A
	Q791R	234,408,177	A/G
	L834P	234,408,306	T/C
	G884R	234,408,455	G/C

Amino acid substitution format is X#Y, where X is the original amino acid, # is the position of the substitution and Y is the new amino acid

exon but downstream of the translation stop codon of *gl15*. Out of 70 HapMap2 SNPs within the *gl15* gene model that vary among the NAM founders, 6 are in the translated region and cause non-synonymous amino acid changes (Supplemental File 1). An SIFT analysis, assessing whether an amino acid substitution affects protein function, showed that none of the six substitutions were predicted to be damaging to *gl15* function with high confidence (Table 2). In addition, SNPs within the *gl15* gene model with minor allele frequency >0.05 were tested for association with expression levels in the shoot apex of 2-week-old seedlings

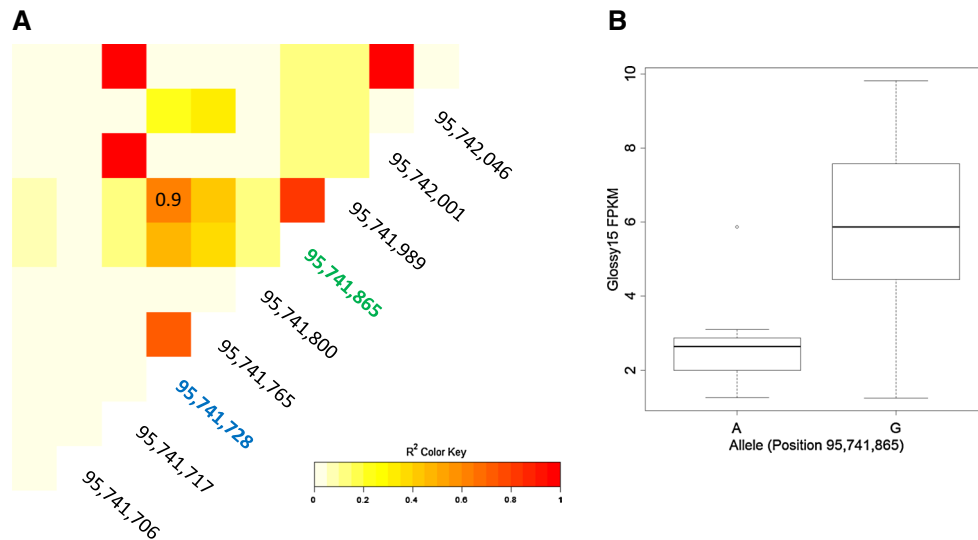


Fig. 5 **a** LD heatmap of 9 SNPs in a 340 bp region in *Glossy15*. Most significant SNP identified by GWAS of LLEW (blue). SNP significantly associated with differences in *Glossy15* expression across

the NAM founder lines (green). **b** Boxplot of *Glossy15* expression in shoot apical meristems of NAM founder lines (Li et al. 2012) by SNP allele at position 95,741,865 on chromosome 9

of the NAM founder lines (Li et al. 2012, qTELLER.com, Supplemental Table 3). One SNP located at 95,741,865 of the 3' UTR is significantly associated with *gl15* expression and passes a Bonferroni multiple test correction ($P = 0.001$). This SNP, associated with *gl15* expression, is in high linkage disequilibrium (LD, $r^2 = 0.9$) with the most significant SNP detected in the NAM GWAS analysis of the last leaf with epicuticular wax (Fig. 5).

GRMZM2G362718 allelic diversity characterization

A similar analysis was done for the chromosome 2 candidate gene, GRMZM2G362718. Out of 27 HapMap2 SNPs within the EDM2-like gene model and segregating among the NAM founder lines, five are non-synonymous changes but none are likely to affect protein function according to an SIFT analysis (Table 2; Supplemental File 2). In addition, SNPs were tested for association with GRMZM2G362718 expression in the shoot apex of 2-week-old seedlings of the 26 NAM founder lines; however, none were significantly associated (Supplemental Table 3).

Discussion

Our study of QTL controlling the juvenile to adult vegetative phase change provides information on the genetic structure of an important developmental trait. We used biparental and NAM populations to map QTLs controlling vegetative phase change and found some concordant regions as well as genomic locations novel to each population/family.

A small number of QTL with major effects underlie the genetic structure of vegetative phase change. This observation is in contrast to another developmental transition, flowering time, which is controlled by many QTL with small effects (Buckler et al. 2009). In fact, many traits evaluated in NAM are controlled by multiple QTL with small effects including leaf architecture, kernel composition and disease resistance (Buckler et al. 2009; Kump et al. 2011; Tian et al. 2011; Cook et al. 2012).

Maize flowering time can be explained by the summation of numerous small, additive QTL. Of the 39 QTL identified using joint-linkage analysis for days to anthesis in the NAM (Buckler et al. 2009), only four were also detected in association with LLEW. Two of the QTL in common are located on chromosome three, one within a flowering time protein and the other in close proximity to an AP2-domain containing protein. This evidence supports the hypothesis that the genetic control of these developmental transitions is independent yet overlapping.

Previous genetic and genomic studies have identified the signaling pathway and miRNA expression cascade involved in the transition of plants from the juvenile to adult vegetative state. By analysis of natural variation that exists for phase change in maize, we were able to map a QTL on chromosome nine where the most significant SNPs in the NAM analysis are located within the candidate gene *gl15*. In addition, *gl15* lies within the confidence interval of the chromosome nine QTL of the IBM analysis. *Glossy15*, identified as a qualitative mutation, is the only cloned gene known to affect vegetative transition in maize (Evans et al. 1994; Moose and Sisco 1994). Our study shows the value of utilizing natural variation to identify alleles of qualitative

mutations that underlie the quantitative variation that exists in populations.

We also identified novel regions of the genome controlling phase change on chromosomes one, two, three, five, eight and seven. The gene model nearest the most significant SNP ($LOD = 212.4$) from single-marker analysis is GRMZM2G362718, located on chromosome two. This SNP is likely extremely significant because B73 contains a unique allele relative to most founders (Fig. 4). While this allele is rare among the founder lines, the B73 genome is represented in 50 % of the NAM population as the common parent among families. This replication of rare alleles in the NAM structure increases the power to detect QTL. GRMZM2G362718 is highly similar to the *enhanced downy mildew 2*-transcription factor of *Arabidopsis*, Rice, Brachypodium, Sorghum, and Grapevine (52.9, 56.7, 42.9, 63.2, 59.5 % similarity, respectively). Several known functions of EDM2-like genes in other species point to its potential significance in underlying the chromosome two QTL. Tsuchiya and Eulgem (2010a, b) reported EDM2 in *Arabidopsis* functions in regulating the vegetative to floral transition in an FLC-dependent manner. Mutations in EDM2 show a delay in flowering and elevated transcripts of the flowering suppressor *FLC* (Tsuchiya and Eulgem 2010a, b). Interestingly, Willmann and Poethig (Willmann and Poethig 2011) showed that *FLC* has both flowering-dependent and flowering-independent effects on vegetative transition in *Arabidopsis*.

EDM2 also has a direct effect on the juvenile to adult vegetative phase change in *Arabidopsis* (Tsuchiya and Eulgem 2010a, b). Similar to other previously identified phase change mutants, *edm2* plants appeared to skip the early juvenile phase of development by not producing the initial pair of rosette leaves. In wild-type *Arabidopsis*, juvenile leaves lack trichomes on the abaxial side, while adult leaves gradually produce more trichomes (Berardini et al. 2001). Mutant *edm2* plants delay the onset of trichome production and, therefore, EDM2 seems to have a role in promoting the transition from the juvenile to adult vegetative phase. This study also included a microarray analysis to determine genes differentially expressed in *edm2* mutants. Tsuchiya and Eulgem found 116 genes whose expression was induced by EDM2 compared to Col-0 wild-type accession and 106 genes suppressed by EDM2. Interestingly, EDM2 does not appear to affect expression of the *trans-acting* siRNAs (*HASTY*, *ZIPPY*, *SGS3*, *RDR6*) or the other five genes (*ARF3*, *ARF4*, *SPL3*, *At1g63130*, *At5g18040*) of this pathway that have previously been shown to control vegetative phase change in *Arabidopsis* (Peragine et al. 2004). This suggests that EDM2's role in vegetative phase change may be independent of the siRNA pathway.

Complementing the NAM analysis, an association analysis was conducted using the Wisconsin Diversity Panel to

detect genomic associations with the last leaf with epicuticular wax (Hirsch et al. 2014). Hirsch et al. (2014) also identified a gene on chromosome 2 (GRMZM2G096016) whose expression at the seedling stage is significantly associated with the juvenile to adult vegetative phase change. GRMZM2G096016 is within the chromosome 2 QTL support interval in this study but not in linkage disequilibrium with the EDM2-like gene, GRMZM2G362718. These findings indicate that there are potentially two different genes that underlie this extremely significant QTL.

This study provides insight into the genetic structure of the juvenile to adult vegetative phase change in maize and identifies individual genes underlying these QTL. Future research can validate the effects of these genes and understand the genetic control of this important developmental trait as well as its overlap in genetic control of the reproductive phase change. Studying the natural variation of developmental transitions has shown to be important for identifying qualitative as well as rare allelic variation. The simplified genetic structure of this trait may prove useful in breeding for either disease resistance or decreased recalcitrance in the context of lignocellulosic ethanol and biofeedstock.

Materials and methods

Genetic materials and phenotypic analysis

QTL discovery was accomplished by analysis of a collection of structured biparental mapping populations. These included the publicly available B73 reference NAM resource (Flint-Garcia et al. 2005) and the IBM RIL mapping population (Lee et al. 2002). Of the ~5,000 NAM RILs, we are only able to maintain adequate seed quantities for field trials of lines that flower in Wisconsin (3875).

The primary trait that was scored to reflect the timing of juvenile to adult transition was the last leaf with juvenile wax. Maize leaves, in order of emergence, can be fully juvenile, part juvenile and part adult (termed transition leaves), and fully adult. Since the earliest emerging juvenile leaves can senesce and become no longer visible at the time that the uppermost transition leaf can be scored, leaf 5 was marked at the young seedling stage (~V7) by punching a hole in the leaf with a leaf punch. At the ~V10 stage, a collar was secured around the stalk between leaf 8 and 9 to mark that internode before the punched leaf 5 fully senesced. The last leaf with juvenile wax was scored on 5 plants per plot with the exact node from which it emerged determined by the position of the leaf collar. At flowering time or thereafter, the total number of leaves (nodes) was determined by counting five plants per plot. Days to pollen shed and days to silk emergence were scored by visual

assessment of the day that 50 % or greater of the plants in a plot had visible pollen shed and visible silk emergence, respectively.

Experimental design and phenotypic data analysis

The NAM families were grown in 2008 and 2009 at the West Madison Agriculture Research Station and the Arlington Agriculture Research Station, respectively. Last leaf with epicuticular wax, days to pollen shed, silk emergence and node number were measured as described above.

The IBM population was grown with two field replications in an RCBD in 2009, 2010, and 2011 at the Arlington Agriculture Research Station (2009, 2010), WI and the West Madison Research Station (2011), WI. Two row plots consisted of 42 plants per plot. Last leaf with epicuticular wax, days to pollen shed, silk emergence and node number were measured as described above.

The following linear model was used for phenotypic analysis of the NAMs:

$$Y_{ik} \sim \mu + P_j + G_{i(j)} + Y_k + e_{ik}$$

where Y is the last leaf with epicuticular wax of the j th population (P) and i th genotype (G) within the j th population in the k th year (Y) and μ is the overall mean. All effects were treated as random.

The following linear model was used for phenotypic analysis of the IBM population:

$$Y_{ijk} \sim \mu + G_i + R_{j(k)} + Y_k + Y_k \times G_i + e_{ijk}$$

where Y is the last leaf with epicuticular wax of the i th genotype (G) in the j th rep (R) within the k th year (Y) and μ is the overall mean. All effects were treated as random.

By-Family repeatabilities in the NAM were calculated as:

$$r^2 = \frac{\sigma^2(G)}{\sigma^2(E) + \sigma^2(G)}$$

where $\sigma^2(G)$ is the genotypic variance and $\sigma^2(E)$ is the error variance (Fehr 1993).

Heritability on an entry mean basis was calculated in the IBM population with the following formula:

$$H^2 = \frac{\sigma^2(G)}{\frac{\sigma^2(E)}{r_y} + \frac{\sigma^2(GY)}{r} + \sigma^2(G)}$$

where $\sigma^2(G)$ is the genotypic variance, $\sigma^2(GY)$ is the genotype by year variance and $\sigma^2(E)$ is the error variance (Fehr 1993).

Significant Pearson and Spearman rank correlations between environments (years and replications) were calculated. Following correlation analysis, means across environments (years for NAM and replications for IBM) were

used for QTL mapping. Phenotypic Pearson correlations were performed for last leaf with epicuticular wax and flowering time, node number, and internode length.

QTL mapping analysis

A set of 1106 single-nucleotide polymorphism (SNP) markers (McMullen et al. 2009) on the 3,875 NAM lines (Buckler et al. 2009) were used for joint linkage mapping by stepwise regression of the LLEW. Because stepwise regression cannot use individuals with missing marker data, an initial step was to impute missing markers. The genetic map is reasonably dense, 1.3 cM average distance between markers (McMullen et al. 2009) and, therefore, double recombination is unlikely. If markers from the same parental genotype flanked a missing marker, the missing marker would be imputed as that parent. B73 alleles were scored as 0 and non-B73 were scored as 2. In the case of different parental genotypes flanking a missing marker, the missing marker was imputed based on proximity to each flanking marker. For example, if the missing marker was 4 cM from a B73 allele and 2 cM from a non-B73 allele, the marker would be scored as 1.5. If the missing marker is exactly half way between different parental markers, a score of 1 was given. Heterozygotes were assigned a value of 1 as well.

In the joint stepwise regression, a population main effect and marker nested within population effect were fit. Using the SAS experimental procedure, GLMSELECT, covariates were determined by forward regression ($P = 0.0001$) and SQL was subsequently used to calculate a likelihood ratio for all markers. A bootstrap analysis was used to determine a genome-wide error rate of 9.10. LOD support interval was calculated as the distance for the significance level to drop 1.5 LOD units on either side of the most significant marker. Additive effects were estimated as half the difference between the phenotypic averages for the two homozygous classes. All allelic effects are relative to B73. The proportion of variation explained by the significant QTL was estimated as the adjusted r^2 of an additive multiple-QTL model.

The 1.6 million SNPs identified in the HapMap1 project (Gore et al. 2009) were imputed in the offspring of the NAM RILs based on founder genotypes (Yu and Buckler 2006; Tian et al. 2011). GWAS was conducted on top of the joint linkage mapping from above. First, residuals for each chromosome were calculated from the full joint linkage model with the removal of any QTL located on that chromosome. Single-marker analysis was then performed on the residuals across all 1.6 million SNPs to determine significance at each locus. A threshold was also set using 1,000 permutations. In addition to single-marker genome scan, a random subsample of 80 % of the RILs from each family was used for forward regression. This was repeated for 100 subsamples to estimate an RMIP, the number of

times a marker appeared in the model across the 100 subsamples, and assess the robustness of the observed associations (Cook et al. 2012). The average of the additive effects and *P* values across subsamples are reported.

A set of 1,340 markers on the recombinant inbred lines of the IBM population (Lee et al. 2002) were used for composite interval mapping with the qtl package of R (Broman et al. 2003). Five marker covariates were used with a window size of 10 cM. One thousand permutations were performed to determine an appropriate significance threshold.

Glossy15 and GRMZM2G362718 allelic diversity analysis

Glossy15 and GRMZM2G362718 protein sequences for each NAM founder were generated based on HapMap2 SNPs (Chia et al. 2012). The SIFT BLink algorithm was used to evaluate non-synonymous amino acid changes on protein function (Kumar et al. 2009). The cloned W64A sequence was used as the functional sequence input of *Glossy15* (GenBank accession GI:1732031, Moose and Sisco 1996) and the B73 reference sequence was used for GRMZM2G362718 (GenBank accession GI: 414592040). *Glossy15* and GRMZM2G362718 expressions on the NAM founder lines were obtained from qTELLER.com (Li et al. 2012; Schnable 2013). A *t* test was used to determine if SNPs within a gene model were significantly affecting levels of expression. Linkage disequilibrium between SNPs was calculated as the allelic correlation (r^2) using the LDheatmap package of R (Shin et al. 2006).

Author contribution statement SMK, NDL and JMF designed the research experiment. JMF and TB collected the data and performed the statistical analysis. JMF, SMK, NDL, and TB wrote the manuscript.

Acknowledgments This work was funded by the DOE Great Lakes Bioenergy Research Center (DOE BER Office of Science DE-FC02-07ER64494). J.F. and T.B. were supported by Monsanto Graduate Fellowships that were a gift to the Plant Breeding and Plant Genetics program at the University of Wisconsin-Madison. We thank William Tracy for his valuable advice.

Conflict of interest The authors declare that they have no conflict of interest.

Ethical standard The experiments comply with the current laws of the United States.

References

Abedon BG, Hatfield RD, Tracy WF (2006) Cell wall composition in juvenile and adult leaves of maize (*Zea mays* L.). *J Agric Food Chem* 54:3896–3900. doi:10.1021/jf052872w

- Berardini TZ, Bollman K, Sun H, Poethig RS (2001) Regulation of vegetative phase change in *Arabidopsis thaliana* by cyclophilin 40. *Science* 291:2405–2407. doi:10.1126/science.1057144
- Bollman KM, Aukerman MJ, Park MY, Hunter C, Berardini TZ, Poethig RS (2003) HASTY, the *Arabidopsis* ortholog of exportin 5/MSN5, regulates phase change and morphogenesis. *Development* 130:1493–1504. doi:10.1242/dev.00362
- Bongard-Pierce DK, Evans MMS, Poethig RS (1996) Heteroblastic Features of Leaf Anatomy in Maize and Their Genetic Regulation. *Int J Plant Sci* 157:331–340. doi:10.1086/297353
- Broman K, Wu H, Sen S, Churchill G (2003) R/qtl: QTL mapping in experimental crosses. *Bioinformatics* 19:889–890. doi:10.1093/bioinformatics/btg112
- Buckler ES, Holland JB, Bradbury PJ, Acharya CB, Brown PJ, Browne C, Ersoz E, Flint-Garcia S, Garcia A, Glaubitz JC, Goodman MM, Harjes C, Guill K, Kroon DE, Larsson S, Lepak NK, Li H, Mitchell SE, Pressoir G, Peiffer JA, Rosas MO, Rocheford TR, Romay MC, Romero S, Salvo S, Sanchez Villeda H, da Silva HS, Sun Q, Tian F, Upadaya N, Ware D, Yates H, Yu J, Zhang Z, Kresovich S, McMullen MD (2009) The genetic architecture of maize flowering time, United States. *Science* 325:714–718. doi:10.1126/science.1174276
- Chia JM, Song C, Bradbury PJ, Costich D, de Leon N, Doebley J, Elshire RJ, Gaut B, Geller L, Glaubitz JC, Gore M, Guill KE, Holland J, Hufford MB, Lai J, Li M, Liu X, Lu Y, McCombie R, Nelson R, Poland J, Prasanna BM, Pyhajarvi T, Rong T, Sekhon RS, Sun Q, Tenaillon MI, Tian F, Wang J, Xu X, Zhang Z, Kaeppler SM, Ross-Ibarra J, McMullen MM, Buckler ES, Zhang G, Xu Y, Ware D (2012) Maize HapMap2 identifies extant variation from a genome in flux, United States. *Nat Genet* 44:803–807. doi:10.1038/ng.2313
- Chuck G, Cigan AM, Saeteurn K, Hake S (2007) The heterochronic maize mutant *Corngrass1* results from overexpression of a tandem microRNA, United States. *Nat Genet* 39:544–549. doi:10.1038/ng2001
- Chuck GS, Tobias C, Sun L, Kraemer F, Li C, Dibble D, Arora R, Bragg JN, Vogel JP, Singh S, Simmons BA, Pauly M, Hake S (2011) Overexpression of the maize *Corngrass1* microRNA prevents flowering, improves digestibility, and increases starch content of switchgrass, United States. *Proc Natl Acad Sci USA* 108:17550–17555. doi:10.1073/pnas.1113971108
- Cook JP, McMullen MD, Holland JB, Tian F, Bradbury P, Ross-Ibarra J, Buckler ES, Flint-Garcia SA (2012) Genetic architecture of maize kernel composition in the nested association mapping and inbred association panels, United States. *Plant Physiol* 158:824–834. doi:10.1104/pp.111.185033
- Evans MM, Passas HJ, Poethig RS (1994) Heterochronic effects of *glossy15* mutations on epidermal cell identity in maize. *Development* 120:1971–1981
- Fehr WR (1993) Principles of Cultivar Development, vol 1. Macmillan Publishing Company, New York
- Gore MA, Chia JM, Elshire RJ, Sun Q, Ersoz ES, Hurwitz BL, Peiffer JA, McMullen MD, Grills GS, Ross-Ibarra J, Ware DH, Buckler ES (2009) A first-generation haplotype map of maize, United States. *Science* 326:1115–1117. doi:10.1126/science.1177837
- Hirsch CN, Foerster JM, Johnson JM, Sekhon RS, Muttoni G, Vailancourt B, Penagaricano F, de Leon N, Kaeppler SM, Buell CR (2014) Insights into the Maize Pan-Genome and Pan-Transcriptome. *Plant Cell* 26:121–135. doi:10.1105/tpc.113.119982
- Huijser P, Schmid M (2011) The control of developmental phase transitions in plants, England. *Development* 138:4117–4129. doi:10.1242/dev.063511
- Kumar P, Henikoff S, Ng PC (2009) Predicting the effects of coding non-synonymous variants on protein function using the SIFT algorithm. *Nat Protoc* 4:1073–1078. doi:10.1038/nprot.2009.86

- Kump KL, Bradbury PJ, Wissner RJ, Buckler ES, Belcher AR, Oropeza-Rosas MA, Zwonitzer JC, Kresovich S, McMullen MD, Ware D, Balint-Kurti PJ, Holland JB (2011) Genome-wide association study of quantitative resistance to southern leaf blight in the maize nested association mapping population. *Nat Genet* 43:163–168. doi:[10.1038/ng.747](https://doi.org/10.1038/ng.747)
- Lawson EJ, Poethig RS (1995) Shoot development in plants: time for a change, England. *Trends Genet* 11:263–268. doi:[10.1016/S0168-9525\(00\)89072-1](https://doi.org/10.1016/S0168-9525(00)89072-1)
- Lee M, Sharopova N, Beavis WD, Grant D, Katt M, Blair D, Hallauer A (2002) Expanding the genetic map of maize with the intermated B73×Mo17 (IBM) population. *Plant Mol Biol* 48:453–461. doi:[10.1023/A:1014893521186](https://doi.org/10.1023/A:1014893521186)
- Li X, Zhu C, Yeh C, Wu W, Takacs EM, Petsch KA, Tian F, Bai G, Buckler ES, Muehlbauer GJ, Timmermans MCP, Scanlon MJ, Schnable PS, Yu J (2012) Genic and nongenic contributions to natural variation of quantitative traits in maize. *Gen Res* 22:2436–2444. doi:[10.1101/gr.140277.112](https://doi.org/10.1101/gr.140277.112)
- McMullen MD, Kresovich S, Villeda HS, Bradbury P, Li H, Sun Q, Flint-Garcia S, Thornsberry J, Acharya C, Bottoms C, Brown P, Browne C, Eller M, Guill K, Harjes C, Kroon D, Lepak N, Mitchell SE, Peterson B, Pressoir G, Romero S, Oropeza Rosas M, Salvo S, Yates H, Hanson M, Jones E, Smith S, Glaubitz JC, Goodman M, Ware D, Holland JB, Buckler ES (2009) Genetic properties of the maize nested association mapping population, United States. *Science* 325:737–740. doi:[10.1126/science.1174320](https://doi.org/10.1126/science.1174320)
- Moose SP, Sisco PH (1994) Glossy15 controls the epidermal juvenile-to-adult phase-transition in maize. *Plant Cell* 6:1343–1355. doi:[10.1105/tpc.6.10.1343](https://doi.org/10.1105/tpc.6.10.1343)
- Moose SP, Sisco PH (1996) Glossy15, an APETALA2-like gene from maize that regulates leaf epidermal cell identity. *Genes Dev* 10:3018–3027
- Nonogaki H (2010) MicroRNA gene regulation cascades during early stages of plant development, Japan. *Plant Cell Physiol* 51:1840–1846. doi:[10.1093/pcp/pcq154](https://doi.org/10.1093/pcp/pcq154)
- Peragine A, Yoshikawa M, Wu G, Albrecht HL, Poethig RS (2004) SGS3 and SGS2/SDE1/RDR6 are required for juvenile development and the production of trans-acting siRNAs in Arabidopsis. *Genes Dev* 18:2368–2379. doi:[10.1101/gad.1231804](https://doi.org/10.1101/gad.1231804)
- Poethig RS (1990) Phase-change and the regulation of shoot morphogenesis in plants. *Science* 250:923–930
- Poethig RS (2003) Phase change and the regulation of developmental timing in plants, United States. *Science* 301:334–336. doi:[10.1126/science.1085328](https://doi.org/10.1126/science.1085328)
- Riedeman ES, Chandler MA, Tracy WF (2008) Divergent recurrent selection for vegetative phase change and effects on agronomic traits and corn borer resistance. *Crop Sci* 48:1723–1731. doi:[10.2135/cropsci2007.09.0511](https://doi.org/10.2135/cropsci2007.09.0511)
- Schnable J (2013) NAM qTeller, <http://qteller.com/NAM>
- Shin J, Blay S, McNeney B, Graham J (2006) LDheatmap: an R function for graphical display of pairwise linkage disequilibrium between single nucleotide polymorphisms. *J Statistical Soft* 23(6):774–776. doi:[10.1093/bioinformatics/btl657](https://doi.org/10.1093/bioinformatics/btl657)
- Tian F, Bradbury PJ, Brown PJ, Hung H, Sun Q, Flint-Garcia S, Rocheford TR, McMullen MD, Holland JB, Buckler ES (2011) Genome-wide association study of leaf architecture in the maize nested association mapping population, United States. *Nat Genet* 43:159–162. doi:[10.1038/ng.746](https://doi.org/10.1038/ng.746)
- Tsuchiya T, Eulgem T (2010a) Co-option of EDM2 to distinct regulatory modules in Arabidopsis thaliana development, England. *BMC Plant Biol* 10:203. doi:[10.1186/1471-2229-10-203](https://doi.org/10.1186/1471-2229-10-203)
- Tsuchiya T, Eulgem T (2010b) The Arabidopsis defense component EDM2 affects the floral transition in an FLC-dependent manner, England. *Plant J* 62:518–528. doi:[10.1111/j.1365-3113.2010.04169.x](https://doi.org/10.1111/j.1365-3113.2010.04169.x)
- van Nocker S, Muszynski M, Briggs K, Amasino RM (2000) Characterization of a gene from Zea mays related to the Arabidopsis flowering-time gene LUMINIDEPENDENS. *Plant Mol Biol* 44:107–122. doi:[10.1023/A:1006472929800](https://doi.org/10.1023/A:1006472929800)
- Willmann MR, Poethig RS (2005) Time to grow up: the temporal role of small RNAs in plants, England. *Curr Opin Plant Biol* 8:548–552. doi:[10.1016/j.pbi.2005.07.008](https://doi.org/10.1016/j.pbi.2005.07.008)
- Willmann MR, Poethig RS (2011) The effect of the floral repressor FLC on the timing and progression of vegetative phase change in Arabidopsis, England. *Development* 138:677–685. doi:[10.1242/dev.057448](https://doi.org/10.1242/dev.057448)
- Yu J, Buckler ES (2006) Genetic association mapping and genome organization of maize, England. *Curr Opin Biotechnol* 17:155–160. doi:[10.1016/j.copbio.2006.02.003](https://doi.org/10.1016/j.copbio.2006.02.003)
- Zotz G, Wilhelm K, Becker A (2011) Heteroblasty—a review. *Bot Rev* 77:109–151. doi:[10.1007/s12229-010-9062-8](https://doi.org/10.1007/s12229-010-9062-8)